



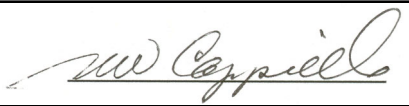
**Document Release
Authorization
To DOE**



Los Alamos National Laboratory

PO Box 1663 MS H816
Los Alamos, NM 87545

This is a milestone document: ☒ **YES** ☐ **NO**

Doc No:	LA-UR-03-7859	Release Date:	10/09/03
Title:	Evaluation of the Control Material Properties of Proposed ADS Structural Materials Before Corrosion Testing in Lead-Bismuth Eutectic		
Author(s):	Stuart Maloy, Subhas Pothana, and Peter Hosemann, Los Alamos National Laboratory		
Approved for Release			
Approved by	Typed Name	Date	Signature
Principal Author:	Stuart A. Maloy	10/09/03	
LANL Program Manager:	Michael W. Cappiello	10/27/03	

Evaluation of the Control Material Properties of Proposed ADS Structural Materials Before Corrosion Testing in Lead-Bismuth Eutectic

1. Introduction

Lead-bismuth eutectic (LBE) has been proposed as an effective coolant for the accelerator-driven systems. Different types of steels are under investigation for their suitability as structural materials in contact with the LBE in the accelerator-driven systems. It was observed that these steels have a tendency to undergo corrosion in a lead-bismuth environment. The rate of this corrosion primarily depends on the oxygen content in the lead-bismuth eutectic, temperature and total time of exposure.

The primary investigation is aimed at evaluating the resistance of various steels (T91, HT-9 (ANL), HT-9 (Timken), 316L, EP-823 (Timken), EP-823 (IPPE), Fe-Si alloys, Fe-Cr alloys, Fe-Si-Cr alloys, pure Fe, Ta, and 316L/T91) to corrosion in the proposed coolant (lead-bismuth eutectic). The materials to be tested are prepared in four different types of specimens, i.e., corrosion, tensile, U-bend, and C-ring specimens. Corrosion specimens are mainly used to evaluate the corrosion by measuring the thickness of the oxide layer formed after testing. Tensile specimens are primarily intended to evaluate the variation of mechanical properties after being exposed to the lead-bismuth eutectic environment. U-bend specimens are mainly intended to observe the combined effect of environment and the induced plastic stress. C-ring specimens are used to observe the combined effect of environment and induced elastic stress.

2. Experimental

The task assigned is focused at evaluating the resistance of 18 different materials (T-91, HT-9 (ANL), HT-9 (Timken), 316L, EP-823 (Timken), EP-823 (IPPE), seven Fe-Si-Cr alloys, three Fe-Si alloys, pure Fe, and a 316L/T91 TIG weld) to corrosion in a proposed lead-bismuth coolant environment. The materials to be tested are initially prepared in two specimen forms. One is a corrosion specimen and the other is a tensile specimen. Some of the specimens are hand-polished to 600 grade, and some are electro-polished. Two polishing methods are employed to observe the effect of polishing on corrosion resistance. These specimens will be exposed for 333-hr, 666-hr, and 1000-hr periods in a flowing lead-bismuth coolant environment (DELTA loop). The materials after testing will be evaluated for the induced corrosion and the variation of mechanical properties.

Accurate, sharp delineation of the true microstructure of materials is of great importance in the characterization of the composition, structure, and properties of materials. One corrosion specimen from each material is picked for the microstructural evaluation. The specimen is cut into three parts and mounted with an epoxy-resin mixture in such a way that all three orthogonal faces of the specimens are exposed for examination (Fig. 1).

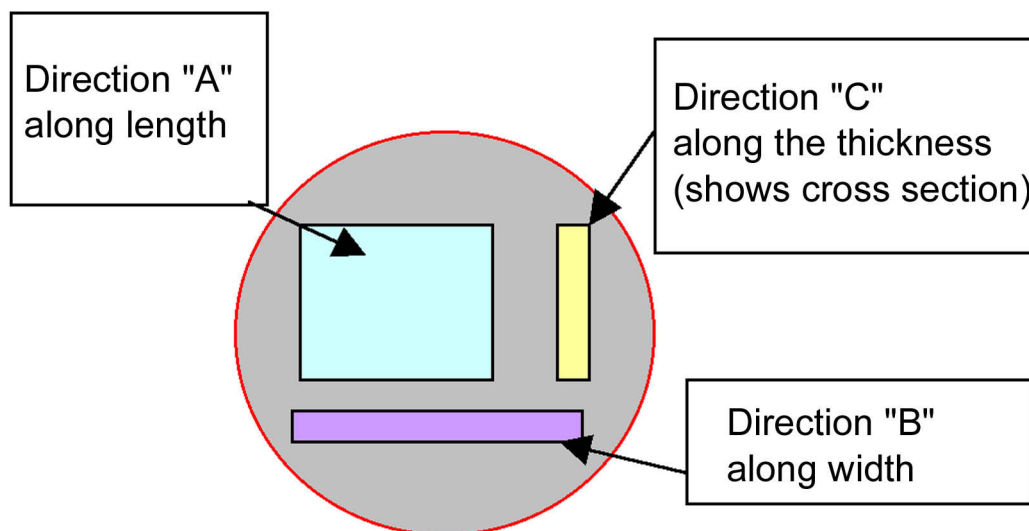


Fig. 1. Diagram showing orientation of specimens in mount.

The polishing of the sample follows sequential steps using 300-grit and 600-grit SiC papers, followed by 15-micron and 1-micron diamond polishing, respectively. For many materials, the microstructure is revealed only by application of an appropriate etchant. To obtain a sharp, delineated, high-contrast condition, the polished surface must be free of any artifacts. The sample must be cleaned thoroughly before etching. A satisfactory etchant must be selected and prepared, and the etching technique must be carefully controlled. The etchant used for the stainless steels was 45 ml HCl, 2.5 ml HNO₃, and 1.5 ml H₂SO₄. The etching time was between 30 seconds and one minute, depending on the material. For the iron, chrome, and silicon alloys, the standard Nitol etching (95% methanol and 5% HNO₃) was used for 15 to 30 seconds.

The microstructures of each specimen were taken at magnifications of 100x, 200x, and 500x, respectively. The grain sizes of the microstructures were evaluated by vertical, horizontal, and circle line techniques, in which four horizontal lines were drawn and the total number of intercepting grains was counted (see Fig. 2).

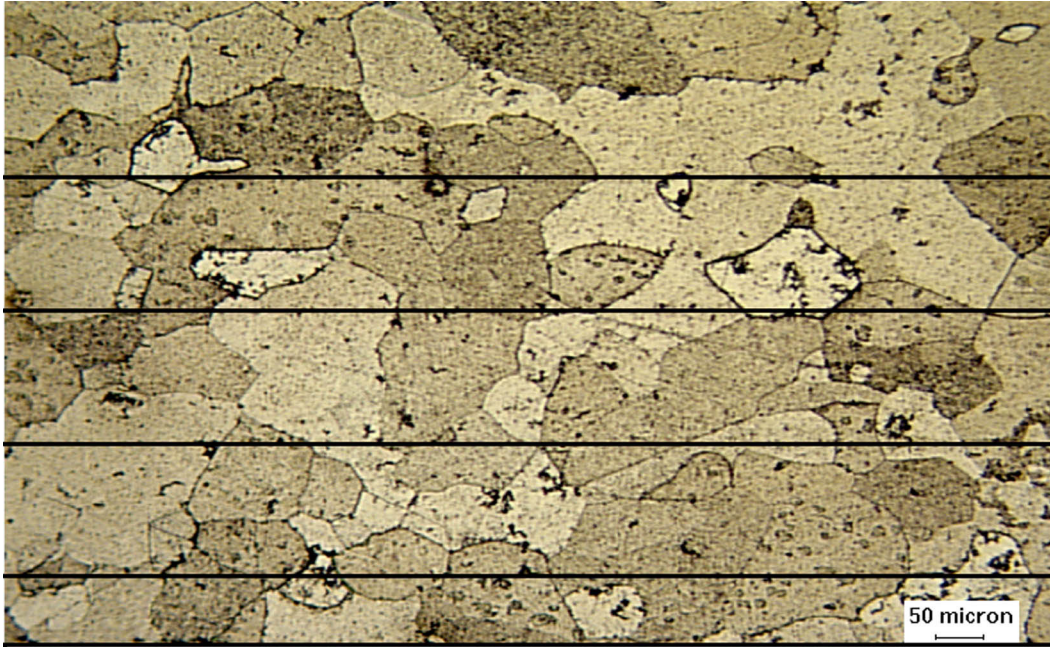


Fig. 2. Line intercept method of measuring grain size. Sample is SiFe-(A).

Then the grain size is calculated by the expression:

Grain size = total length of the vertical or horizontal lines/total number
of intercepts of grain boundaries $\times 1.125$.

The microhardness of each material was measured by a Vickers hardness testing machine. The microhardness measurement was done after the metallographic analysis in the microscope, because in this way it was possible to select the microhardness measuring spots depending on the grain structure. At the measurement location, a diamond pyramid indenter is loaded into the material. The size of the impression shown on the material after this process indicates the hardness. The two diagonal lengths horizontal (d_1) and vertical (d_2) of the indentation formed were measured. The applied load is known. In this microhardness testing machine, a fixed load (L) of 0.5 kg was applied. The Vickers hardness number (HV) is measured by expression

$$HV = 1.854L/d^2 \text{ [kg/mm}^2\text{]}$$

where d = Mean diagonal $(d_1 + d_2)/2$ and L = Load (kg).

In addition to the material samples two weld samples were analyzed. Both specimens were a TIG weld between the materials T91 and 316L.

3. Evaluation of Mechanical Properties

The tensile properties of the engineering materials [T-91, HT-9 (ANL), HT-9 (Timken), 316L, EP-823 (Timken)] were tested in tension before exposure in the lead-bismuth loop. The specimen used had a flat dogbone shape. The dimensions of the gage length were ~3.1 mm wide, 1 mm thick, and 13 mm long. An average of three dimensional measurements on each specimen was used for calculating stress and strain. All the specimens were pulled at a strain rate of 1×10^{-3} per second in tension. Two specimens were tested for each alloy at room temperature. The data points such as load, time, extensometer reading, and crosshead position were recorded. From the obtained values of load and extensometer reading, the engineering stress (σ_e) vs. engineering strain (e) and true stress (σ_t) vs. true strain (ϵ) were plotted using the following expressions.

$$\sigma_t = \sigma_e \times (1+e)$$

$$\epsilon = \ln(1+e)$$

The yield stress was measured as the intersection of a line at an offset of 0.2% of engineering strain parallel to the linear elastic region in the engineering stress vs. engineering strain plot. The same plot was used to determine the ultimate tensile stress, uniform elongation, and final elongation. The uniform elongation here is the engineering strain at ultimate tensile stress. The obtained mechanical properties were tabulated as shown in Table 6 later in this report.

4. Data

Table 1. Elemental Composition of the Analyzed Materials

Material	Cr wt%	Si wt%	Ni wt%	C wt%	Mo wt%	Mn wt%
1	1	—	—	—	—	—
2	2.25	—	—	—	—	—
3	9	—	—	—	—	—
4	12	—	—	—	—	—
6	2.25	0.5	—	—	—	—
7	2.25	1.25	—	—	—	—
8	12	0.5	—	—	—	—
SiFe(A)	0.09	1.24	0.08	0.01	—	—
SiFe(B)	0.08	2.55	0.15	0.02	—	—
SiFe(C)	—	3.82	—	0.01	—	—
pure iron	—	—	—	—	—	—
T91	8.26	0.3	0.13	0.1	0.95	0.38
EP-823	12	1.3	0.8	0.18	0.9	0.8
HT-9	11.5	0.4	0.5	—	—	0.6
316L	17.3	0.35	12.1	0.02	2.31	1.8



Table 2. Grain Size Analysis of the Corrosion Specimens

Image	Total Length (μm)	Intercepts	Average Grainsize (μm)	Average Overall Measurements (μm)
1-A-x100-001cir	4884.84	80	68.69	°
1-B-x100-002 cir	4884.84	89	61.75	°
1-B-x100-002 hor	4254.03	60	79.76	°
1-B-x100-002 ver	3071.39	85	40.65	62.71
	°	°	°	°
2-A-x100-001 cir	4884.84	77	71.37	°
2-B-x200-005 cic	2482.00	49	56.98	°
2-B-x200-005 hor	2107.00	40	59.26	°
2-B-x200-005 ver	1560.72	40	43.90	57.88
	°	°	°	°
3-A-x100-001cir	4884.84	91	60.39	°
3-C-x100-005cir	4884.84	102	53.88	57.13
	°	°	°	°
4-A-x100-001 cir	4884.84	97	56.65	°
4-B-x100-003 cir	4884.84	105	52.34	°
4-B-x100-003 hor	4254.00	71	67.40	°
4-B-x100-003 ver	3071.00	69	50.07	56.62
	°	°	°	°
6-A-x100-001cir	4884.84	88	62.45	°
6-C-x100-005 cir	4884.84	69	79.64	°
6-C-x100-005 hor	4254.00	65	73.63	°
6-C-x100-005 cir	3071.00	60	57.58	68.33
	°	°	°	°
7-A-x100-001 cir	4884.84	124	44.32	°
7-C-x100-008 cir	4884.84	85	64.65	54.49
	°	°	°	°
8-A-x100-001 cir	4884.84	108	50.88	°
8-B-x100-003 cir	4884.84	118	46.57	48.73
	°	°	°	°
SiFeA-A-x100-001 cir	4884.84	62	88.64	°
SiFeA-C-x100-004 cir	4884.84	73	75.28	81.96
	°	°	°	°
SiFeB-A-x100-001 Cir	4884.84	121	45.42	°
SiFeB-A-x100-001 hor	4254.03	60	79.76	°
SiFeB-A-x100-001 ver	3071.39	85	40.65	°
SiFeB-B-x200-004 cir	2482.00	114	24.49	°
SiFeB-B-x200-004 hor	2107.00	54	43.90	46.84
	°	°	°	°
SiFeC-A-x100-001 cir	4884.84	14	392.53	°
SiFeC-C-x100-003 cir	4884.84	29	189.50	291.01



Image	Total Length (μm)	Intercepts	Average Grainsize (μm)	Average Overall Measurements (μm)
Pure Iron-A-x100-001 cir	4884.84	133	41.32	
Pure Iron-B-x200-002 Cir	2492.27	120	23.37	
Pure Iron-B-x200-002 hor	2107.00	46	51.53	
Pure Iron-B-x200-002 ver	1560.00	101	17.38	33.40
316L-A x100 hor.	4254	185	25.87	
316L-A x100 vert.	3169	102	34.95	
316L-B x100 hor.	4254	154	31.08	
316L-B x100 vert.	3071	89	38.82	31.71
EP-823 (IPEE)-Ax200-hor	2107	280	8.47	
EP-823 (IPEE)-Ax200-vert	1560	241	7.28	
EP-823 (IPEE)-Bx200-hor	2107	164	14.45	
EP-823 (IPEE)-Bx200-vert	1560	207	8.48	9.67
EP-823 (Timken)-Ax200-hor	2107	213	11.13	
EP-823 (Timken)-Ax200-ver	1560	150	11.70	
EP-823 (Timken)-Bx200-hor	2107	229	10.35	
EP-823 (Timken)-Bx200-ver	1560	197	8.91	10.52
HT-9 (ANL)-Ax100-hor	4254	211	22.68	
HT-9 (ANL)-Ax100-vert	3071	146	23.66	
HT-9 (ANL)-Bx200-hor	2107	131	18.09	
HT-9 (ANL)-Bx200-vert	1560	78	22.50	21.73
HT-9 (Timken)-Ax100-hor	4254	262	18.27	
HT-9 (Timken)-Ax100-vert	3071	181	19.09	
HT-9 (Timken)-Bx100-hor	4254	107	44.73	
HT-9 (Timken)-Bx100-vert	3071	80	43.19	31.32
T-91-Ax100-hor	4254	191	25.06	
T-91-Ax100-vert	3071	136	25.40	
T-91-Bx100-hor	4254	133	35.98	
T-91-Bx100-vert	3071	111	31.13	29.39



Table 3. Microhardness Analysis of the Corrosion Specimens

Material	Direction	Avg Hardness (MPa)
316L	A	138.4
°	B	139.4
°	C	146.6
EP-823 (IPEE)	A	363.1
°	B	381.0
°	C	351.2
EP-823(Timken)	A	260.9
°	B	259.8
°	C	265.6
HT-9 (ANL)	A	281.9
°	B	246.8
°	C	233.4
HT-9 (Timken)	A	260.9
°	B	239.8
°	C	248.0
T-91	A	249.0
°	B	246.8
°	C	233.4
1	A	68.9
°	B	95.1
2	A	62.9
°	B	85.8
3	A	90.6
°	B	106.4
4	A	99.1
°	B	116.0
6	A	93.9
°	B	117.2
7	A	120.4
°	B	133.8
8	A	136.1
°	B	137.7
SiFe-A	A	156.2
°	B	146.4
SiFe-B	A	269.5
°	B	274.0
SiFe-C	A	248.6
°	B	258.2
Pure Fe	A	140.9
	B	136.8



Table 4. Microhardness Analysis of the T91-316L Weld

	HV of the Hand-Polished Specimen	HV of the Electro-Polished Specimen
Location 1	172.5	173.2
Location 2	182.6	181.1
Location 3	168.4	174.4
Location 4	156.7	160.1
Location 5	170.7	164.6
Location 6	231	216.7
Location 7	275.6	315
Location 8	248.3	222.8

Table 5. Weight and Thickness Measurements

Material	MID	SID	Weight Before Testing (gm)	Thickness Before Testing (mm)
EP-823 (Timken)	1110	1010	2.0564	0.981
EP-823 (IPEE)	11001	0010	2.0875	0.9963
HT-9 (Timken)	0110	0001	1.9124	0.8977
HT-9 (ANL)	1100	1101	2.05	0.9653
316L	1010	0100	2.1252	0.9607
T91	1000	01001	1.9644	0.924
1	00011	001	2.1806	1.009
2	00101	101	2.1776	1.009
3	00010	010	2.15	1.0185
4	00000	101	2.1733	1.0125
6	00001	001	2.1473	1.015
7	10001	101	2.1648	1.0165
8	01001	110	1.963	0.906
SiFeA	01000	100	1.8957	0.908
SiFeB	01110	001	1.8997	0.908
SiFeC	10010	010	1.9153	0.893
Pure Iron	01010	100	2.0404	0.889



Table 6. Tensile Properties of the Engineering Alloys

Material	No.	σ_y (MPa)	S_u (MPa)	e_u (mm/mm)	e_t (mm/mm)
316L	1	219	608	0.59	0.67
	2	219	607	0.59	0.67
EP-823 (Timken)	1	573	799	0.102	0.172
	2	599	799	0.102	0.180
HT9 (ANL)	1	640	855	0.088	0.145
	2	650	852	0.073	0.125
HT9 (Timken)	3	626	773	0.096	0.150
	4	605	750	0.100	0.150
T-91	1	601	734	0.068	0.131
	2	527	740	0.082	0.142

Key to abbreviations:

σ_y : 0.2% offset yield stress.

S_u : Engineering ultimate tensile stress.

e_u : Uniform elongation.

e_t : Total elongation.



**Fig. 3. Photomicrograph
of 316L (100x).**



**Fig. 4. Photomicrograph
of EP-823 (IPPE) (100x).**



**Fig. 5. Photomicrograph
of EP-823 (Timken) (200x).**

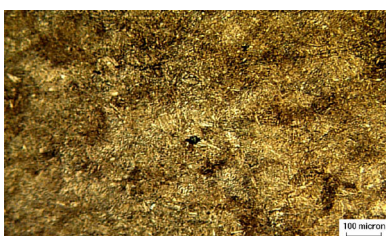


**Fig. 6. Photomicrograph
of HT-9 (ANL)-A 100x.**

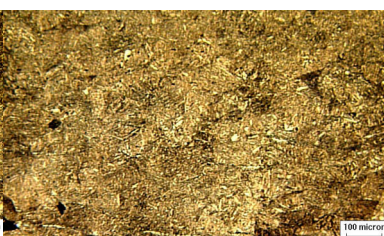


**Fig. 7. Photomicrograph
of HT-9 (Timken) 100x.**

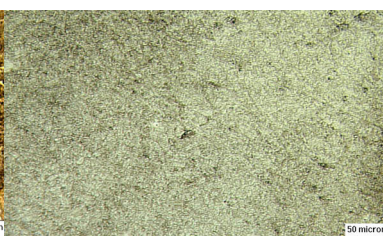


**Fig. 8. Photomicrograph
of T91 (ANL)-A x100.**

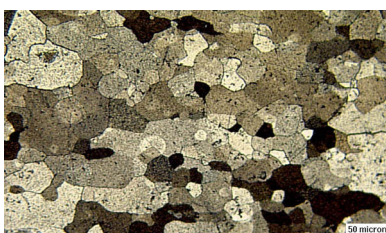


**Fig. 9. Photomicrograph
of material 1-A x100.**

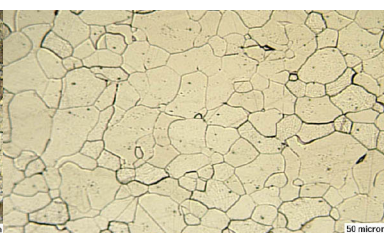


**Fig. 10. Photomicrograph
of material 2-A x100.**

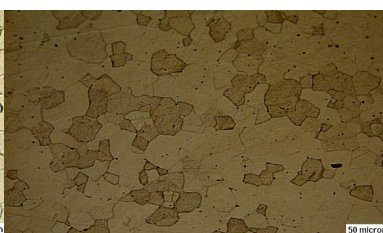


**Fig. 11. Photomicrograph
of material 3-A x100.**

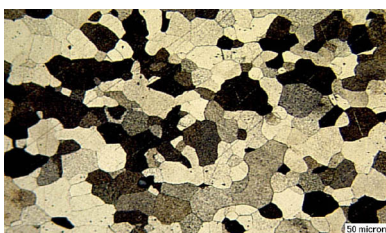


**Fig. 12. Photomicrograph
of material 4-A x100.**

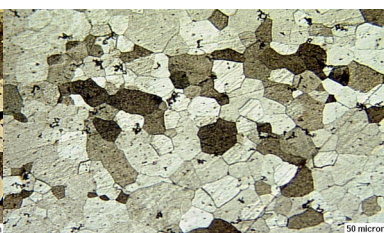


**Fig. 13. Photomicrograph
of material 6-A x100.**

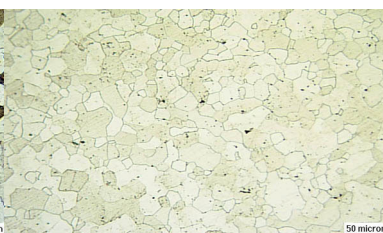


**Fig. 14. Photomicrograph
of material 7-A x100.**

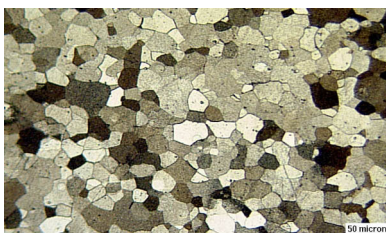


**Fig. 15. Photomicrograph
of material 8-A x100.**

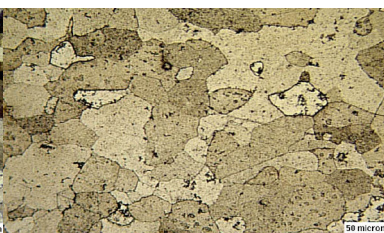


**Fig. 16. Photomicrograph
of SiFe(A)-A x100.**

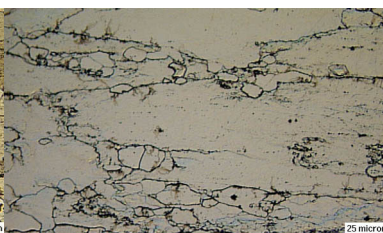


**Fig. 17. Photomicrograph
of SiFe(B)-A x200.**

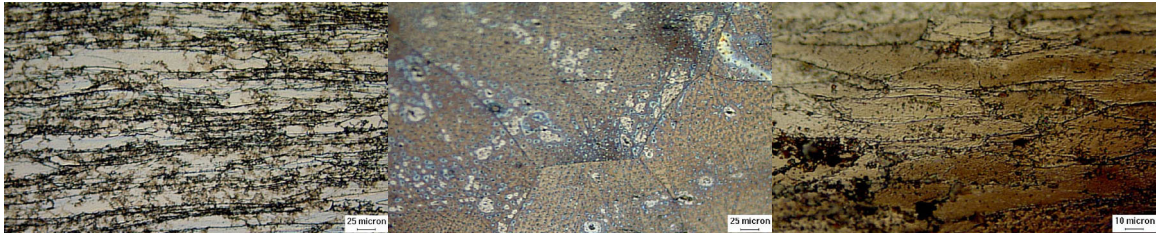


**Fig. 18. Photomicrograph
of SiFe(B)-C $\times 200$.**

**Fig. 19. Photomicrograph
of SiFe(C)-C $\times 200$.**

**Fig. 20. Photomicrograph
of pure iron-A $\times 200$.**

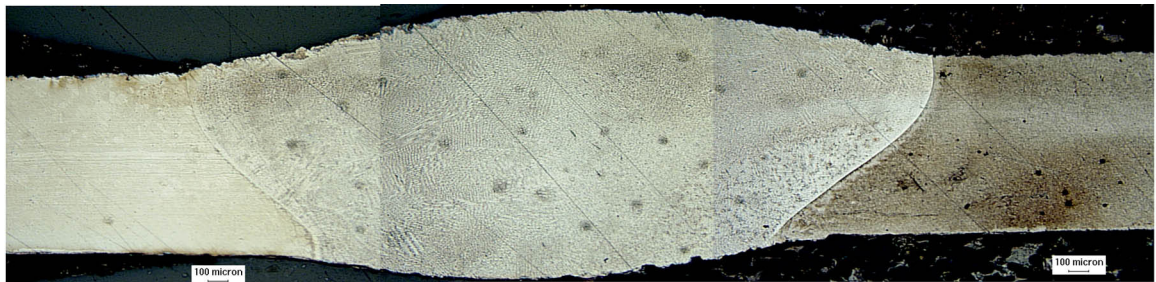


Fig. 21. Photomicrograph showing the grain structure of a TIG weld between 316L and T91. The austenitic (316L) material is on the left side, and the ferritic/martensitic material (T91) is on the right side. The cast structure in the weld comes mostly from the filler, IN82.

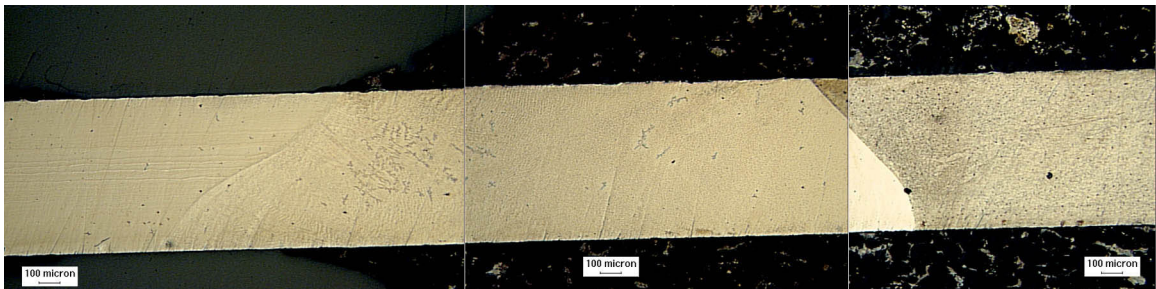


Fig. 22. Photomicrograph showing the grain structure of a TIG weld between 316L and T91 after polishing to remove the weld bead. The Austenitic (316L) material is on the left side the and the ferritic/martensitic material(T91) is on the right side. The cast structure in the weld comes mostly from the filler, IN82.

5. Discussion

The samples T91, HT-9 (ANL), HT-9 (Timken) and EP-823 (Timken) had the same heat treatment. The heat treatment after the rolling process was a solution heating at 1038°C for 1 hr and air cooling after that, followed by aging heating at 760°C for 1 hr with air cooling after this heating.

We found that these materials HT-9 (ANL) (Fig. 6), and HT-9 (Timken) (Fig. 7), T91 (ANL) (Fig. 8), and EP823 (Timken) had typical tempered martensitic structures. The material EP823 (IPPE) had a typical rolled microstructure as it was not heat-treated. It was analyzed in the as-received condition. The 316L material showed an equiaxed grain structure, with annealing twins typical of an annealed austenitic structure. No rolling structure was visible in this material. The alloys 1, 2, 3, 4, 6, 7, 8, and SiFe(A) showed no rolling structures, but the material SiFe(C) and pure Fe showed strong rolling structures.

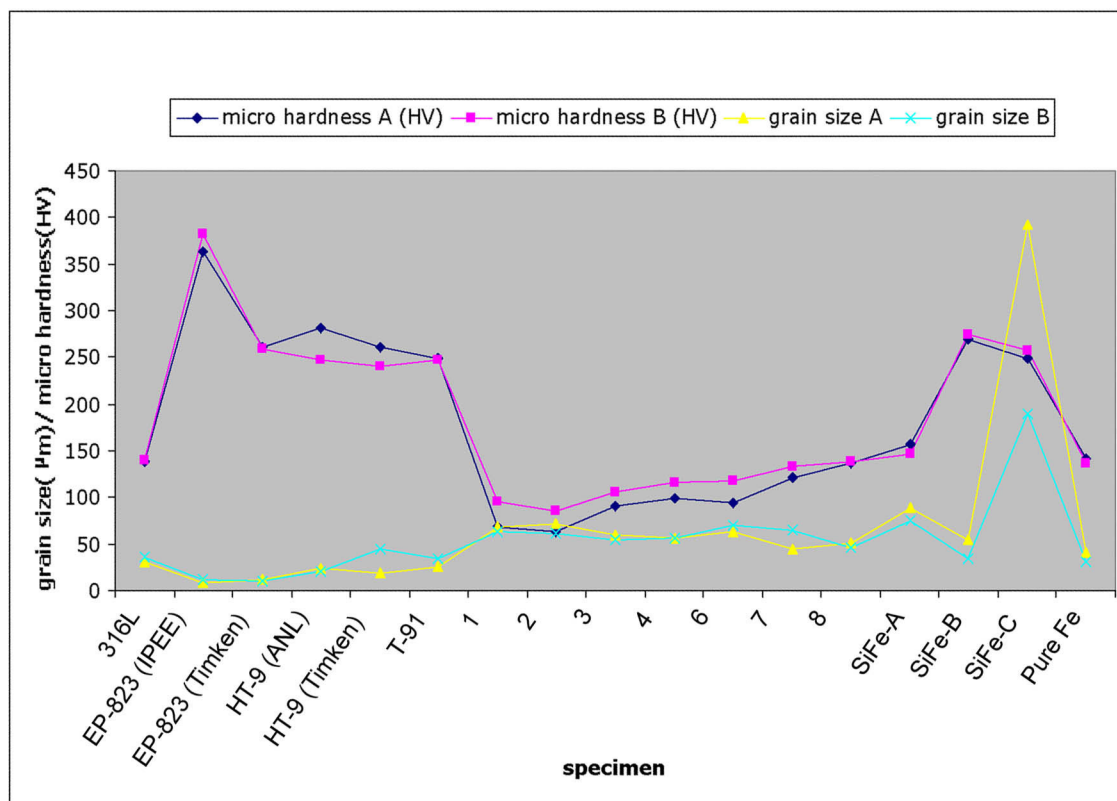


Fig. 23. Microhardness and grain size.

In Fig. 23 the microhardness measurements and the grain size are shown in one diagram. In general, this diagram shows that materials with a small grain size have higher microhardness. An exception to this rule is observed in the Si-Fe(C) alloy. It has a

very large grain size but also a high hardness because of the strong work hardening that occurred during rolling.

The hardness of the 316L/T91 TIG weld specimen is shown in Fig. 24. A decrease in hardness is observed in the welding zone and a maximum in hardness is observed in the bulk material in the weld-heat-affected zone. The hardness in the center of the weld is a cast grain structure from mainly filler material, IN 82, which is not martensitic and has a large grain size leading to a softer material. At the T91 bulk material side where the heat-affected zone is located, a very large hardness is observed. This can be explained because fast cooling occurs in this zone. This produced a fine martensitic structure that results in an increased hardness. Also in this area is some residual stress from the welding process that leads to an increase in the hardness. The effect of the high residual stresses is observed in the heat-affected zone on the 316L side of the weld as well. In this case, the hardening effect is not as large because no martensite is formed as the high nickel content in this alloy prevents the martensite formation.

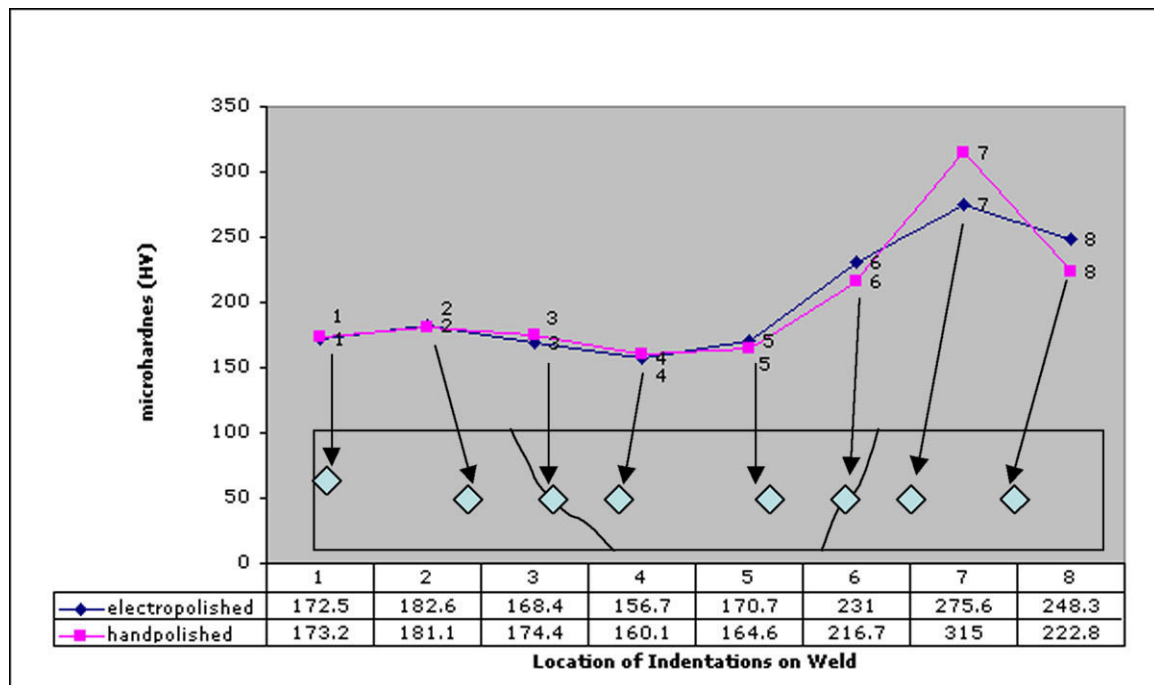


Fig. 24. Microhardness measurements on T91/316L weld.

The engineering and true stress/strain curves for the alloys [T-91, HT-9 (ANL), HT-9 (Timken), 316L, EP-823 (Timken)] are shown in Figs. 25—28. The largest ductility is obtained with annealed 316L stainless steel. Because of the large ductility on this material, the extensometer had to be unloaded at around 30% plastic strain to be able to test the specimens to failure. That is why first and second loading can be seen in Fig. 25. For the rest of the alloys (T-91, HT-9, and EP-823), similar values of yield stress, ultimate stress, and uniform elongation were observed. A slightly higher yield stress was

observed for the HT-9 (ANL) alloy. This agrees with the slightly elevated hardness observed for this alloy as well.

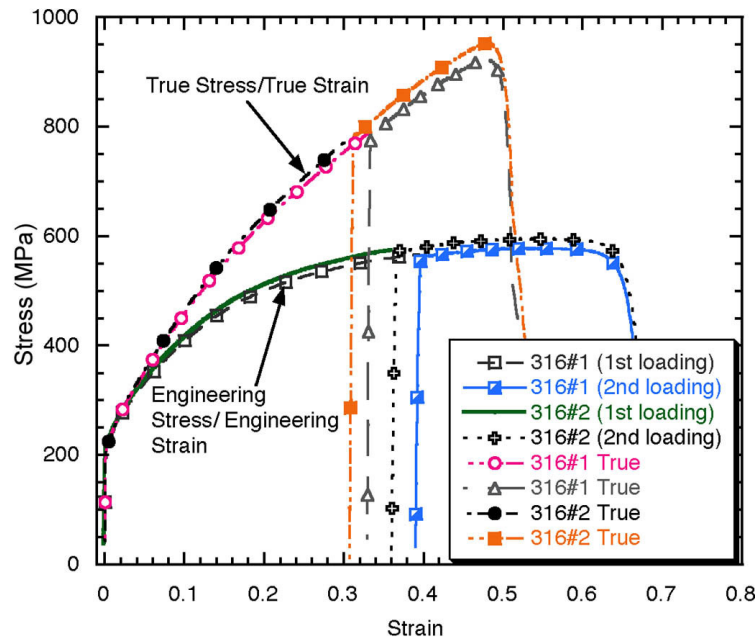


Fig. 25. Tensile stress/strain curves for annealed 316L stainless steel specimens. Specimen was unloaded between first and second loading to reset extensometer.

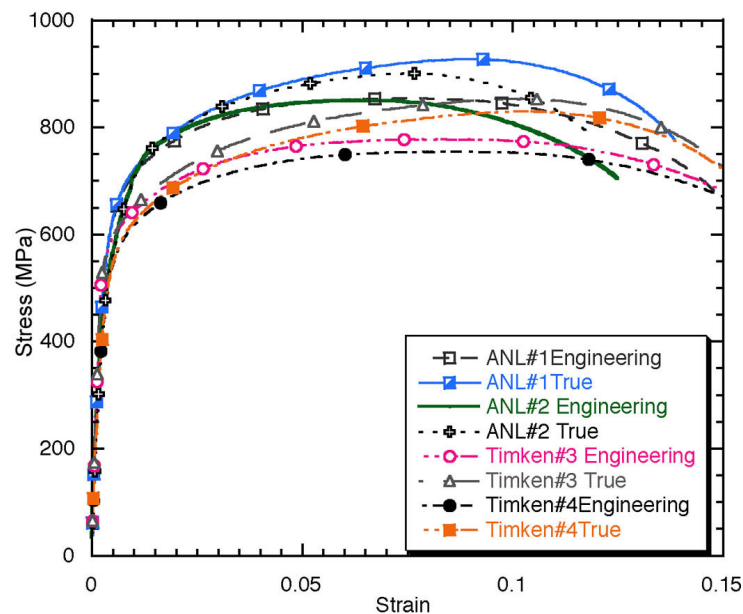


Fig. 26. Tensile stress/strain curves for normalized and tempered HT-9 specimens.

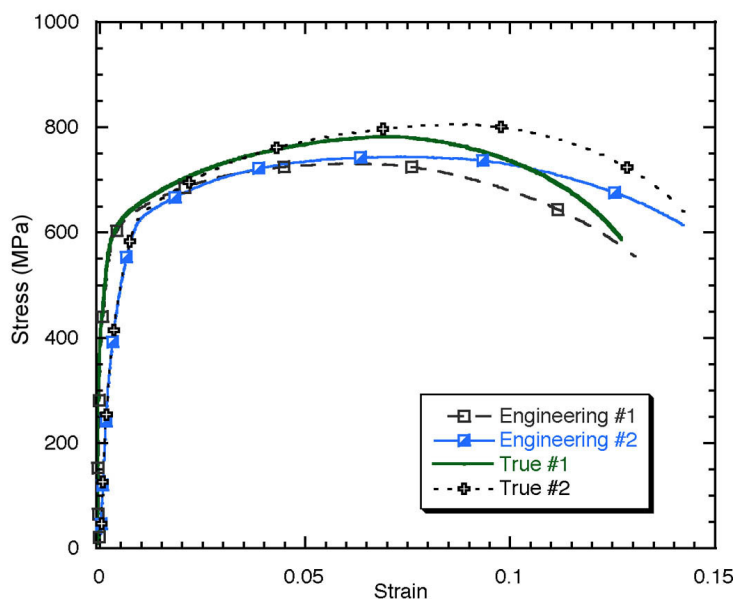


Fig. 27. Tensile stress/strain curves for normalized and tempered T91 specimens.

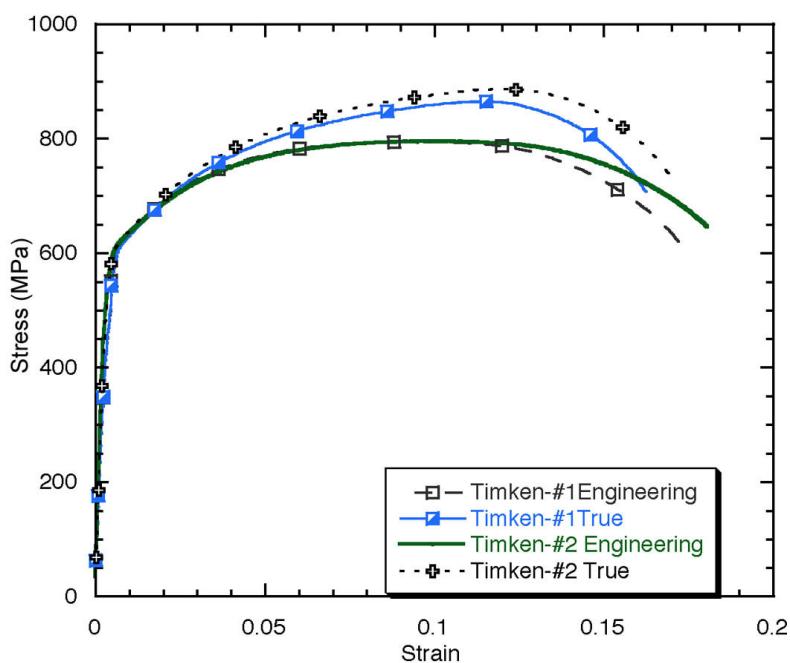


Fig. 28. Tensile stress/strain curves for normalized and tempered EP-823 specimens.



6. Conclusions

This report summarized the control properties of engineering and experimental alloys to be tested in corrosion in the DELTA lead-bismuth loop. The microstructures were analyzed using optical microscopy, and Vickers microhardness was measured. In addition, to test for possible liquid-metal embrittlement and mechanical property changes, the tensile properties of the engineering alloys (HT-9, EP-823, 316L, and T91) were measured.